Tellus (1987), *39A*, 202–214

Favorable environments for explosive cyclogenesis in a modified two-layer Eady model

By H. Y. WENG[1] and A. BARCILON[1,2], *Florida State University, Tallahassee, Florida 32306, USA*

(Manuscript received 2 July; in final form 17 October 1986)

ABSTRACT

A modified two-layer Eady model is used to find favorable environments for explosive cyclogenesis by examining baroclinic instability of both short and long waves. The model includes Ekman dissipation and low-level sensible heating, and allows both static stabilities and vertical shears to be different but constant in each layer. It is found that an enhanced low-level shear, a reduced low-level static stability, a relatively large upper-level static stability, and an appropriate height of the interface are favorable for the short-wave development, and that an enhanced upper-level shear and a relatively small upper-level static stability are favorable for the long-wave development, while having opposite effects on the short wave. A small Ekman dissipation is favorable for the development of both waves. Newtonian sensible heating does not directly enhance the development of both waves. A favorable environment for explosive cyclogenesis may not be expressed by a single parameter, but rather by a combination of baroclinic instability with several parameters which contribute collectively to the development of both short and long waves. The relative phase of these waves also plays an important part: the development is enhanced when the surface cyclone is ahead of the upper level wave trough by $\frac{1}{2}\pi$.

1. Introduction

Baroclinic instability is probably one of the dominant mechanisms for the development of most explosively deepening cyclones. Sanders and Gyakum (1980), who studied explosive cyclogenesis in the Northern Hemisphere during the period September 1976–May 1979, showed that these cyclones occurred over a wide range of sea surface temperature (SST), but preferentially near the strongest surface gradients. Hanson and Long (1984) analyzed cyclogenesis occurring off the east coast of China for the period 1879–1962, and revealed that the strong north-south gradient of SST across the East China Sea played a significant role in winter cyclogenesis. They suggested that the surface baroclinicity associated with this temperature gradient was the dominant mechanism for this kind of cyclogenesis. Roebber (1984) found that the preferred regions of explosive cyclogenesis were primarily baroclinic zones which supported the development and continued existence of ordinary low pressure systems. Rogers and Bosart (1986) recently analyzed North Atlantic and Pacific weather ship rawinsonde data and also found that for most explosively deepening cyclone, ordinary baroclinic instability is probably the dominant mechanism for their development. Although these works did not preclude the possibility that, in some strong storm cases, the rapidity of the development may be strongly enhanced by the cumulus convection associated with CISK-like mechanism described by many authors (Rasmussen, 1979; Gyakum, 1983) and recently modelled by Wang and Barcilon (1986) in a simple analytic model, a combination of the ordinary baroclinic process in conjunction with other "dry" effects has attracted more and more attention in studying the mechanism of explosive cyclogenesis. These effects include the approach of an upper-level planetary

[1] Geophysical Fluid Dynamics Institute.
[2] Department of Meteorology.

trough, the low static stability found in the lower layer and the thickness of that layer, the reduced roughness of the sea surface, the tropopause folding, and probably the sensible heating, etc.

Frederiksen (1979), by using a linear, two-layer quasi-geostrophic model, studied the effect of planetary waves on the regions of cyclogenesis. He found that the upper layer long wave had little effect on the growth rate and phase speed of the fastest growing mode; however, it played an important rôle in producing regions of preferential development downstream of the long-wave troughs closest to the pole. These results were consistent with the observational study by Blackmon (1976). Sanders and Gyakum (1980) further revealed that most explosive cyclones which occurred over the northwest Atlantic and Pacific were about 640 km downstream from a mobile 500 mb trough, within or poleward of the maximum westerlies, and within or ahead of the planetary-scale trough. This flow situation for explosive cyclogenesis over northwest oceans was also found over the northeast Pacific where no strong warm ocean current exists. Mullen (1983) found that there was a simultaneous development of the disturbance aloft. The trough at 500 mb had sharpened considerably while the trough at 850 mb had closed off. Intensification of the system as it entered the region just downstream of the planetary wave trough was consistent with Frederiksen's (1979) theoretical work. Murty et al. (1983) found a similar relationship between upper- and low-level systems in a case study of explosive cyclogenesis in the northeast Pacific. When the upper trough gradually caught up, a closed low formed over the surface low and maximum deepening occurred. The overtaking of the deepening surface center by a mobile 500 mb trough was similar to Petterson's scenario (1956). Sanders (personal communication) recently found a high correlation between upper-level cyclonic vorticity advection over the surface cyclone and simultaneous surface deepening rate, and concluded that the explosive cyclone appears to be a fundamentally baroclinic disturbance in which the low-level response to a given upper-level forcing is extremely large. Thus, when we examine the mechanisms of explosive cyclogenesis, we should consider those mechanisms which cause both the surface low- and the upper-level planetary trough to develop.

The effect of sensible heat on the development of cyclones is controversial. The presence of the Kuroshio and the Gulf Stream are responsible for the fact that the east coasts of Asia and North America are two of the most favored regions for cyclogenesis. During periods of strong outbreaks of cold continental air, the sensible heat transfer at the air-sea interface reaches very large values. Min and Horn (1974) used the bulk aerodynamic method to estimate the generation of available potential energy by sensible heating along the east coasts of Asia and North America, and found that it was of about the same size as the hemispheric values for all diabatic processes obtained by other investigators. They pointed out the importance of sensible heating in cyclogenesis in these regions. Nevertheless, Hanson and Long (1984) concluded that air-sea temperature difference and averaged heat fluxes showed little relationship to the cyclogenesis. By using the same kind of bulk aerodynamic method in which the heating is of the Newtonian form, Haltiner (1965) showed that this type of diabatic heating reduced the instability of short and medium waves and shifted the maximum instability to a shorter wave length than the corresponding adiabatic model; however, the instability of long waves was increased. Fisher and Winn-Nielsen (1971) considered the effect of the diabatic heating having Newtonian form on baroclinic instability of ultra-long waves. They found that the perturbation instability was decreased by Newtonian heating. Mansfield (1974) also found that heating from the sea surface reduced the growth rate. We want to determine if sensible heating has a positive or a negative direct effect on the development of cyclogenesis.

The fact that even a rough sea surface induces less frictional dissipation than land may be a favorable factor for intensive development of extratropical cyclones in a maritime environment. Sanders and Gyakum (1980) found that cyclogenesis occurred in a relatively smooth area of the sea state from observational data. Danard and Ellenton (1980) numerically showed that the contrast in frictional drag was responsible for cyclone deepening over water while under similar conditions no deepening would take place over land.

The thickness of the lower layer may also be important for the development of a disturbance with a certain scale. Saito (1977) compared cases of developed and non-developed depressions over the East China Sea. In the case of non-developed depressions, the region with low static stability was confined to the layer below 700 mb, whereas in the central part of a developed depression, the region with low static stability extended from the surface up to 500 mb, showing that such a depression has a deeper favorable environment than a non-developed depression. Staley and Gall (1977) and Blumen (1979), by using a four-level geostrophic model and a two-layer Eady model, respectively, studied short-wave baroclinic instability. Staley and Gall (1977) dealt with the effects of the low-level static stability and vertical shear. Blumen (1979) showed how sensitive the short-wave instability was to the relative depths of the layers and the low-level static stability.

We extend Blumen's model, where long and short wave instabilities may coexist, to include sensible heating and Ekman dissipation, and allow both static stabilities and vertical shears to be different but constant in each layer, and propose to use this model as a guide to understand favorable explosive cyclogenesis environments. We first discuss the factors which are favorable for the development of short and long waves, respectively. Then, we seek an idealized synoptic environment favorable for explosive cyclogenesis to analyze the rôle of the various mechanisms.

2. The model

We consider a two-layer, two-dimensional, quasi-geostrophic, Boussinesq fluid in an x-z plane. There are bottom and top Ekman layers with different strengths, the top one being one tenth that of the bottom. The lower layer is favorable for the development of short waves. The basic flows in both layers are westerlies and vary linearly only with height, with constant but different shear in each layer. The Coriolis parameter is constant; the Brunt-Väisälä frequencies are constant but different in each layer. The sensible heating is assumed to be proportional to the difference between the perturbation temperature of the air at the bottom of the atmosphere, T_a', and the perturbation temperature of the underlying surface, T_s', having assumed that the air and the ground are in thermal equilibrium averaged along the x-axis. Since the temperature of the air is one of the dependent variables, the heating is dependent on the motion. Observations indicate that the major part of the heating takes place below 700 mb (Winston, 1965; Haltiner, 1965). Thus, we limit the heating in the lower layer and assume that the upper layer is adiabatic. The sensible heating function is chosen as

$$Q' = K'(T_s' - T_a')\left(1 - \frac{z'}{H'}\right), \tag{2.1}$$

where K' is the dimensional heating constant, which is taken as 10^{-2} m^2 s^{-3} as used by Haltiner (1965). H' is the dimensional height of the interface and z' is the dimensional vertical coordinate. The upper and lower layers are linked by the requirement that total pressure and vertical velocity are continuous at the interface $z' = H'$. The flow is periodic in x' direction. The parameters representing the lower layer and the upper layer carry subscripts $_1$ and $_2$, respectively.

Let D denote the total depth, 0 and U represent the basic velocity at the bottom and the top, respectively, N_1 and N_2 be Brunt-Väisälä frequencies in the low- and upper-level, respectively, and take the Coriolis parameter as $f_0 = 1.03 \times 10^{-4}$ s^{-1}. To nondimensionalize the equations use $U = 20$ m s^{-1} as a velocity scale, $D = 10^4$ m as a vertical scale, $L = 10^6$ m as a horizontal scale, L/U as a time scale, and UL as a scale for the geostrophic stream function. Then, the nondimensional perturbation potential vorticity equations in each layer are

$$\left(\frac{\partial}{\partial t} + U_1\frac{\partial}{\partial x}\right)\left(\nabla^2\phi_1 + \frac{1}{S_1}\frac{\partial^2\phi_1}{\partial z^2}\right) = \frac{1}{S_1}\frac{\partial Q}{\partial z}, \tag{2.2a}$$

$$\left(\frac{\partial}{\partial t} + U_2\frac{\partial}{\partial x}\right)\left(\nabla^2\phi_2 + \frac{1}{S_2}\frac{\partial^2\phi_2}{\partial z^2}\right) = 0, \tag{2.2b}$$

and the vertical boundary conditions and the matching conditions are

$$\left(\frac{\partial}{\partial t} + U_1\frac{\partial}{\partial x}\right)\frac{\partial\phi_1}{\partial z} - \frac{\partial U_1}{\partial z}\frac{\partial\phi_1}{\partial x} + \delta\nabla^2\phi_1 = Q, \quad \text{at } z = 0, \tag{2.3a}$$

$$\left(\frac{\partial}{\partial t} + U_2\frac{\partial}{\partial x}\right)\frac{\partial\phi_2}{\partial z} - \frac{\partial U_2}{\partial z}\frac{\partial\phi_2}{\partial x} - \rho\delta\nabla^2\phi_2 = 0, \quad \text{at } z = 1, \tag{2.3b}$$

$$\phi_1 = \phi_2, \qquad \text{at } z = H, \tag{2.3c}$$

$$\left(\frac{\partial}{\partial t} + U_1 \frac{\partial}{\partial x}\right)\frac{\partial \phi_1}{\partial z} - \frac{\partial U_1}{\partial z}\frac{\partial \phi_1}{\partial x} = \alpha^{-2}\left[\left(\frac{\partial}{\partial t} + U_2 \frac{\partial}{\partial x}\right)\frac{\partial \phi_2}{\partial z} - \frac{\partial U_2}{\partial z}\frac{\partial \phi_2}{\partial x}\right], \qquad \text{at } z = H, \tag{2.3d}$$

where

$$S_i = \frac{N_i^2 D^2}{f_0^2 L^2}, \quad \text{for } i = 1, 2,$$

$$\alpha = \frac{N_2}{N_1}, \qquad Q = -K\left(1 - \frac{z}{H}\right)\frac{\partial \phi_1}{\partial z}\bigg|_{z=0},$$

$$\delta = \frac{E_1^{1/2}}{2R_0} S_1, \qquad \rho = \frac{E_2^{1/2} S_2}{E_1^{1/2} S_1},$$

and H is the nondimensional height of the interface, ϕ_i, U_i, S_i are nondimensional streamfunction of perturbation field, basic velocity and stratification parameter in the layer i, respectively. K is the constant which is given by

$$K = \frac{K' L}{c_p U},$$

where $c_p = 9.96 \times 10^2\ \mathrm{m^2\ K^{-1}\ s^{-2}}$ and K is about 0.5. U_1 and U_2 are expressed by

$$U_1 = \lambda_1 z,$$

$$U_2 = \lambda_1 H + \lambda_2 (z - H),$$

where λ_i $(i = 1, 2)$ is the vertical shear in layer i. E_i and R_0 are the Ekman number of the layer i and the Rossby number, respectively. ρ is assumed to be 0.1.

The solutions of ϕ_1 and ϕ_2 are of the form

$$\phi_1(x, z, t) = \psi_1(z)\, e^{ik(x - ct)}, \tag{2.4a}$$

$$\phi_2(x, z, t) = \psi_2(z)\, e^{ik(x - ct)}. \tag{2.4b}$$

The governing equations for ψ_1 and ψ_2 are

$$\frac{d^2 \psi_1}{dz^2} - \mu_1^2 \psi_1 = -\frac{c_H}{(\lambda_1 z - c) H}\frac{d\psi_1}{dz}\bigg|_{z=0}, \tag{2.5a}$$

$$\frac{d^2 \psi_2}{dz^2} - \mu_2^2 \psi_2 = 0, \tag{2.5b}$$

$$(c + c_H)\frac{d\psi_1}{dz} + (\lambda_1 - ik\delta)\psi_1 = 0, \text{ at } z = 0, \tag{2.5c}$$

$$[c - \lambda_1 H - \lambda_2 (1 - H)]\frac{d\psi_2}{dz} + (\lambda_2 + ik\rho\delta)\psi_2 = 0, \qquad \text{at } z = 1, \tag{2.5d}$$

$$\psi_1 = \psi_2, \qquad \text{at } z = H, \tag{2.5e}$$

$$(\lambda_1 H - c)\frac{d\psi_1}{dz} - \lambda_1 \psi_1 = \alpha^{-2}\left[(\lambda_1 H - c)\frac{d\psi_2}{dz} - \lambda_2 \psi_2\right], \qquad \text{at } z = H, \tag{2.5f}$$

where

$$\mu_1 = k\sqrt{S_1}, \qquad \mu_2 = k\sqrt{S_2}, \qquad c_H = i\frac{K}{k},$$

and c_H represents the effect of the sensible heating. The potential vorticity in the upper layer, where no heat source exists, is conserved, while that in the lower layer changes following a fluid particle due to diabatic heating. Thus, ψ_1 is a combination of the common solution without heating and a particular solution with heating, i.e.,

$$\psi_1 = \psi_{1c} + \psi_{1p}. \tag{2.6}$$

Then, the solutions of (2.5a, b) which satisfy (2.5c–f) are

$$\psi_{1c}(z) = A_1 \cosh(\mu_1 z) + B_1 \sinh(\mu_1 z), \tag{2.7a}$$

$$\psi_{1p}(z) = B_1 \frac{c_H}{a_0 \lambda_1 H}\left[I_s(z)\cosh\left(\mu_1 z - \frac{\mu_1}{\lambda_1}c\right) - I_c(z)\sinh\left(\mu_1 z - \frac{\mu_1}{\lambda_1}c\right)\right], \tag{2.7b}$$

$$\psi_2(z) = A_2 \cosh(\mu_2 z) + B_2 \sinh(\mu_2 z), \tag{2.7c}$$

where

$$I_s(z) = \sum_{n=0}^{\infty} \frac{\left(\mu_1 z - \frac{\mu_1}{\lambda_1}c\right)^{2n+1}}{(2n+1)(2n+1)!},$$

$$I_c(z) = \ln(\lambda_1 z - c) + \sum_{n=0}^{\infty} \frac{\left(\mu_1 z - \frac{\mu_1}{\lambda_1}c\right)^{2n}}{2n(2n)!},$$

$$a_0 = 1 + \frac{c_H}{\lambda_1 H}\left[I_c(0)\cosh\left(\frac{\mu_1}{\lambda_1}c\right) + I_s(0)\sinh\left(\frac{\mu_1}{\lambda_1}c\right)\right].$$

The relations between A_1, B_1, A_2 and B_2 are given in the Appendix.

The eigenvalue c can be obtained by substituting (2.7a–c) into (2.5c–f). The dispersion relation has a complicated form, and is given in the Appendix.

3. Analysis of different effects on growth rates

In this section, we examine the effects of some physical factors on growth rates and the wavelengths of the most unstable short wave and long wave, respectively. These factors are the vertical shears λ_1 and λ_2, the stratification parameters S_1 and S_2, the height of the interface H, the strength of the Ekman dissipation δ, and the strength of the sensible heating K. Under certain conditions, there are two unstable regions. For convenience, we define the wavenumber of the most unstable long planetary and short synoptic waves as k_{mp} and k_{ms}, respectively.

3.1. A case of Blumen's

We use one of Blumen's cases as our control case; it is characterized by $S_1 = 1.0$, $S_2 = 1.21$, $\lambda_1 = 1.0$, $\lambda_2 = 1.0$, $K = 0.0$, $\delta = 0.0$, and $H = 0.3$ and is shown in Fig. 1. For the most unstable long and short waves $k_{\mathrm{mp}} = 1.5$ and $k_{\mathrm{mp}} c_i = 0.28$, and $k_{\mathrm{ms}} = 3.4$ and $k_{\mathrm{ms}} c_i = 0.15$, respectively. The long-wave instability is very similar to the wave instability in the one-layer Eady model. The parameters used here may be viewed as representative of the early stages of baroclinic wave development within the troposphere.

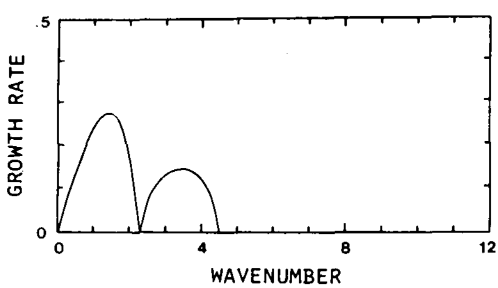

Fig. 1. The growth rate in a Blumen's case where $S_1 = 1.0$, $S_2 = 1.21$, $\lambda_1 = 1.0$, $\lambda_2 = 1.0$, $K = 0.0$, $\delta = 0.0$, and $H = 0.3$.

3.2. The effects of low-level and upper-level shears

Fig. 2a shows the dependence of the growth rate on wavenumber and low-level shear λ_1 when $S_1 = 1.0$, $S_2 = 1.21$, $\lambda_2 = 1.0$, $K = 0.0$, $\delta = 0.0$, and $H = 0.3$. The shadowed area represents the stable region. The short wave instability is greatly enhanced by increasing λ_1. As λ_1 doubles, k_{ms} increases slightly from 3.4 to 3.5, while $k_{\mathrm{ms}} c_i$ increases from 0.15 to 0.45. The long-wave instability is slightly enhanced by the low-level shear.

Fig. 2b shows the dependence of the growth rate on wavenumber and upper-level shear λ_2 when $S_1 = 1.0$, $S_2 = 1.21$, $\lambda_1 = 1.0$, $K = 0.0$, $\delta = 0.0$, and $H = 0.3$. The variation of λ_2 has opposite effects on long-wave and short-wave instabilities. When λ_2 increases from 1.0 to 2.0, $k_{\mathrm{mp}} c_i$ increases from 0.28 to 0.53, while $k_{\mathrm{ms}} c_i$ substantially decreases. In this case, the short wave instability is almost suppressed when $\lambda_2 > 1.3$.

3.3. The effects of low-level and upper-level static stabilities

Fig. 3a gives the dependence of the growth rate on wavenumber and low-level stratification parameter S_1 for $S_2 = 1.21$, $\lambda_1 = 1.0$, $\lambda_2 = 1.0$, $K = 0.0$, $\delta = 0.0$, and $H = 0.3$. Both k_{ms} and $k_{\mathrm{ms}} c_i$ increase as S_1 decreases, while both k_{mp} and $k_{\mathrm{mp}} c_i$ are almost invariant. k_{mp} is about 1.5 and $k_{\mathrm{mp}} c_i$ is close to 0.28, while k_{ms} increases from 3.4 to 5.2 and $k_{\mathrm{ms}} c_i$ increases from 0.15 to 0.37, as S_1 decreases from 1.0 to 0.5. Thus, the reduction of the low-level static stability greatly affects the short wave instability, a result consistent with observations and some theoretical findings (Staley and Gall, 1977; Blumen, 1979; Anthes et al., 1983).

Comparing Figs. 2a and 3a, we see that the effect of increasing λ_1 on growth rate of the most unstable short wave is more efficient than the effect of decreasing S_1. According to the analysis of Hanson and Long (1984), the initial position of storm formation is controlled by baroclinic instability processes which in turn depend strongly on north-south sea surface temperature gradients that are responsible for the formation of large low-level shear.

Fig. 3b exhibits the dependence of the growth rate on wavenumber and upper-level stratification parameter S_2 when $S_1 = 1.0$, $\lambda_1 = 1.0$, $\lambda_2 = 1.0$, $K = 0.0$, $\delta = 0.0$, and $H = 0.3$. It is seen

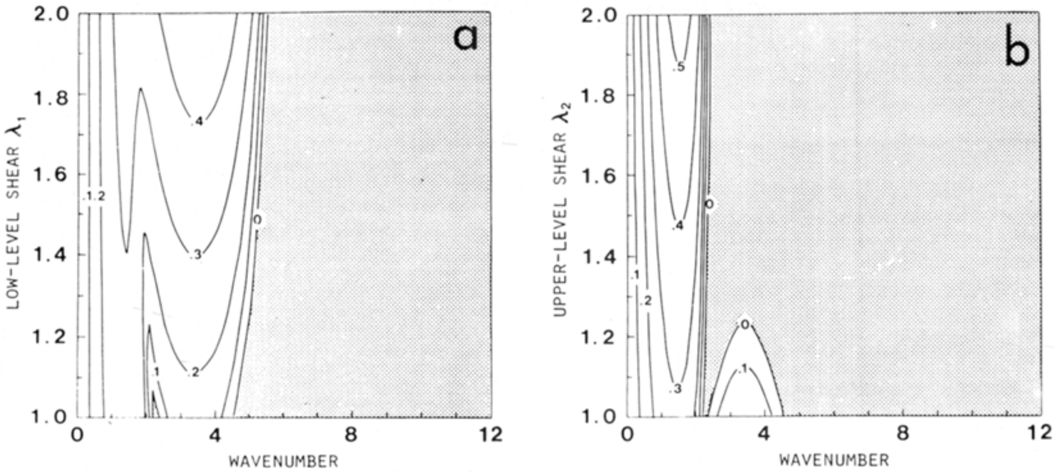

Fig. 2. The dependence of the growth rate on wavenumber and (a) low-level shear λ_1 for $\lambda_2 = 1.0$, and (b) upper-level shear λ_2 for $\lambda_1 = 1.0$, when $S_1 = 1.0$, $S_2 = 1.21$, $K = 0.0$, $\delta = 0.0$ and $H = 0.3$. The shadowed areas in Figs. 2–4 represent stable regions.

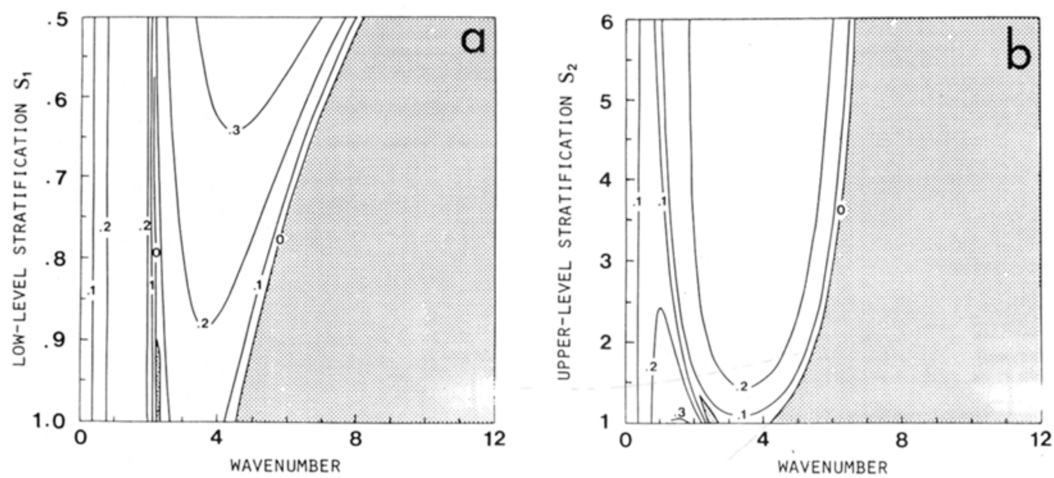

Fig. 3. The dependence of the growth rate on wavenumber and (a) low-level stratification parameter S_1 for $S_2 = 1.21$, and (b) upper-level stratification parameter S_2 for $S_1 = 1.0$, when $\lambda_1 = 1.0$, $\lambda_2 = 1.0$, $K = 0.0$, $\delta = 0.0$, and $H = 0.3$.

that the variation of upper-level static stability has opposite effects on long and short wave instabilities. In the long wave unstable region, both k_{mp} and $k_{mp} c_i$ decrease as S_2 increases. Nevertheless, in the short wave unstable region, both k_{ms} and $k_{ms} c_i$ increase as S_2 increases. As S_2 increases from 1.1 to 6.0, k_{ms} increases slightly from 3.4 to 4.1, while $k_{ms} c_i$ increases substantially from 0.15 to 0.30. There is a jump of instability between $S_2 = 1.0$ where only long wave instability exists, and $S_2 > 1.0$ where both long-wave and short-wave instabilities coexist. This is because the model reduces to the one-layer Eady model when $S_2 = 1.0$. The results suggest that for $H < 0.5$ the high upper-level static stability is conducive to the development of short waves, while it suppresses the development of the long waves. This effect is prominent in the range between $S_2 = 1.0$ and 2.0. The result is in agreement with Blumen's (1979), but differs from that of Staley and Gall (1977), who concluded that changing the static stability in the upper layer would not have much effect on the short waves. Nevertheless, observations and some numerical results do show the above effect on the low-level short wave instability (Hoskins, 1971; Uccellini et al., 1985).

3.4. The effect of the height of the interface

Fig. 4a shows the dependence of growth rate on wavenumber and height of the interface when $S_1 = 1.0$, $S_2 = 1.21$, $\lambda_1 = 1.0$, $\lambda_2 = 1.0$, $K = 0.0$, and $\delta = 0.0$. Since $S_2 > S_1$ and $\lambda_1 = \lambda_2$, there is no short wave instability for $H > 0.5$. For $H < 0.5$, the unstable region is divided into two regions, each having its own maximum growth rate. In the long wave unstable region, k_{mp} is kept at 1.5–1.6 and $k_{mp} c_i$ is kept at 0.28–0.30, while in the short wave unstable region, $k_{ms} c_i$ is around 0.15 and k_{ms} becomes larger as the lower layer becomes shallower. Thus, the height of the interface alone does not have much influence on the growth rate of both long and short waves, but it greatly affects the wavenumber of the most unstable short wave, k_{ms}.

Figs. 4b and 4c give the dependence of growth

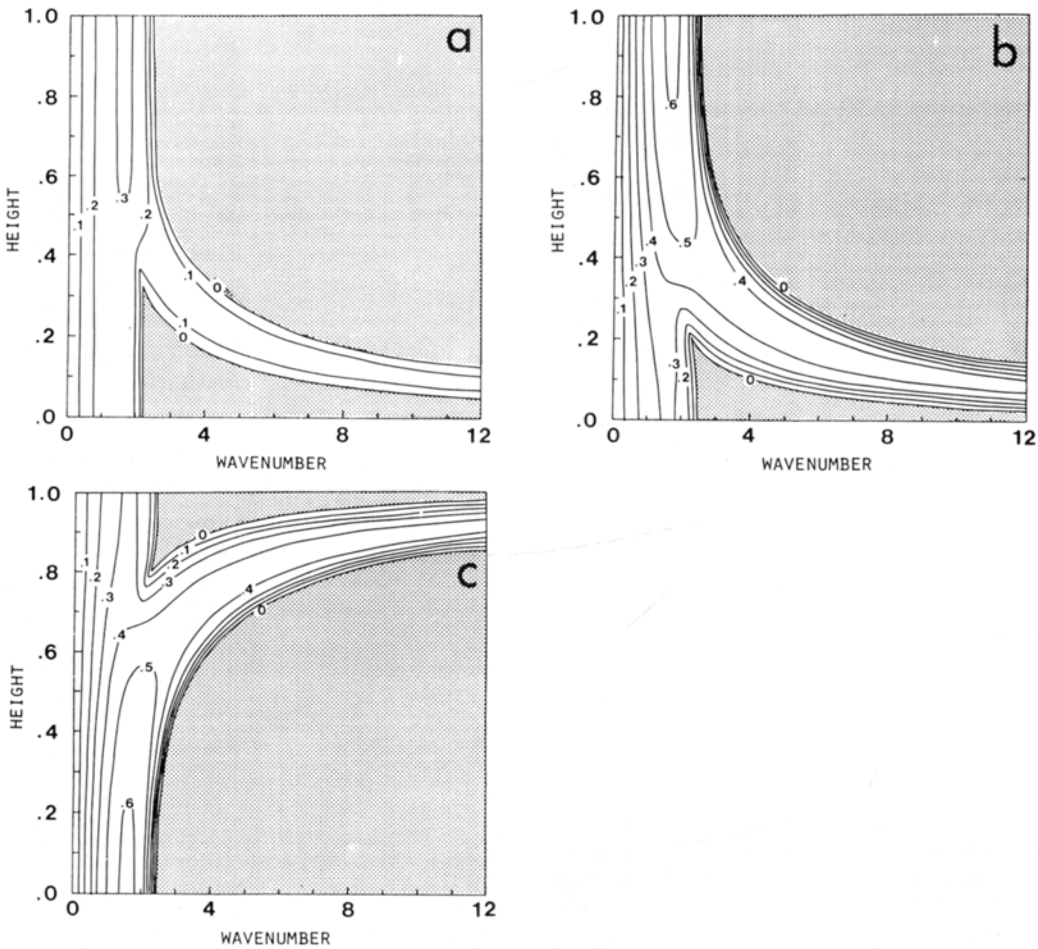

Fig. 4. The dependence of the growth rate on wavenumber and height of the interface for (a) $S_1 = 1.0$, $S_2 = 1.21$, $\lambda_1 = 1.0$, $\lambda_2 = 1.0$, (b) $S_1 = S_2 = 1.0$, $\lambda_1 = 2.0$, $\lambda_2 = 1.0$, and (c) $S_1 = S_2 = 1.0$, $\lambda_1 = 1.0$, $\lambda_2 = 2.0$, when $K = 0.0$, and $\delta = 0.0$.

rate on wavenumber and height of the interface when $\lambda_1 = 2.0$ and $\lambda_2 = 1.0$, and $\lambda_1 = 1.0$ and $\lambda_2 = 2.0$, respectively, with $S_1 = S_2 = 1.0$. Comparing the results shown in Figs. 4b and 4c, it is seen that the vertical variation of vertical shear may play a rôle in the wavenumber selection. For $H < 0.5$, $\lambda_1 > \lambda_2$ is favorable for the development of short waves, while $\lambda_1 < \lambda_2$ is favorable for the development of long waves; for $H > 0.5$, the effect is opposite. Although Blumen (1979) kept both $\lambda_1 = \lambda_2 = 1$, he found the possibility that the variation of shears would have similar effects with those due to the vertical variation of stratification.

3.5. The effect of Ekman dissipation

Fig. 5a shows the effect of Ekman layer suction on growth rate when $S_1 = 1.0$, $S_2 = 2.0$, $\lambda_1 = 1.0$, $\lambda_2 = 1.0$, $K = 0.0$, $H = 0.3$, and when $\delta = 0.0$, 0.01, and 0.1. As δ is increased, i.e., as the Ekman dissipation is increased for fixed S_1, the growth rates of most wavenumbers are reduced and the wavenumbers of the most unstable long and short waves shift to the smaller wavenumbers. With friction the waves grow considerably less rapidly and much less efficiently, except for very short waves which are shorter than the cut-off wavelength in the inviscid case. This effect may partly explain why a cyclone originating on east China mainland and moving seaward often intensifies when over water. Even a rough sea surface exhibits less surface drag than dry land and favors cyclogenesis (Sanders and Gyakum, 1980).

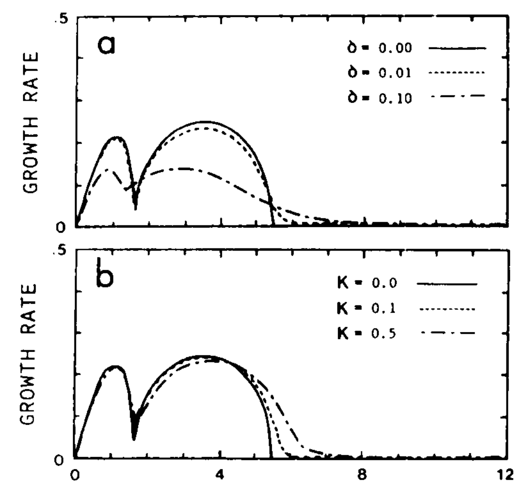

Fig. 5. (a) The effect of Ekman dissipation on the growth rate for $K = 0.0$, and (b) the effect of sensible heating with Newtonian form for $\delta = 0.0$, when $S_1 = 1.0$, $S_2 = 2.0$, $\lambda_1 = 1.0$, $\lambda_2 = 1.0$ and $H = 0.3$.

3.6. The effect of sensible heating with Newtonian form

Fig. 5b shows the effect of sensible heating, parameterized by means of a Newtonian form, on the growth rates when $S_1 = 1.0$, $S_2 = 2.0$, $\lambda_1 = 1.0$, $\lambda_2 = 1.0$, $\delta = 0.0$, $H = 0.3$ and when $K = 0.0$, 0.1, and 0.5. This kind of heating stabilizes the longer waves, destabilizes the very short waves, and moves the short wave cut-off to very large wavenumbers, as seen in Fig. 5b. This result is consistent with those obtained by Fisher and Wiin-Nielsen (1971) and Mansfield (1974), and that of Haltiner (1965) except for that the latter author found that, in his model, the instability of long waves was increased. Thus, the sensible heating, when parameterized by means of a Newtonian form, does not directly provide a positive feedback for the development of both planetary and synoptic waves. Yet, in nature, sensible heating may indirectly play an important role in the pre-development stage of cyclogenesis by reducing the low-level static stability, S_1, an effect which we studied through variations of that parameter. Comparing Figs. 5a and 5b, it is seen that the dissipation effect due to sensible heating is not as large as that of Ekman pumping.

4. Favorable environments for explosive cyclogenesis and rôles of the various mechanisms

Explosive cyclogenesis occurs in a complex environment in which many conditions must be met. By examining the rôle of different parameters, the previous section gives a better understanding of conditions favorable for the development of short and long waves. Since sensible heat is a minor factor compared with Ekman dissipation, it could be neglected for our purpose. We can envisage of a favorable environment for explosive cyclogenesis in which the most unstable short and long waves have large growth rate, or one in which the short wave rapidly develops while the long wave coexists with it.

Fig. 6a is an example of the environment for a non-developing cyclone. It is the Bluemen's case to which Ekman dissipation of $\delta = 0.1$ has been added. There is a fairly strong long-wave instability and a very weak short-wave instability. The growth rate of the most unstable long wave is about 0.20 which corresponds to an e-folding time of 2.9 days. Its wavenumber is 1.4 corresponding to a wavelength of 4,500 km or about 6 waves around the latitude circle at 45°N. The growth rate of the most unstable short wave is about 0.06 which corresponds to an e-folding time of 9.7 days. Its wavenumber is 3.0 which corresponds to a wavelength of 2,100 km. In fact, this short wave should be neglected, since its growth rate is less one third that of the most unstable long wave. This environment can be expressed by the following parameters. The low-level static stability corresponds to a lapse rate of 6.8 K km^{-1} for the mean temperature of 280 K. The upper-level static stability corresponds to a lapse rate of 6.5 K km^{-}. The mean wind is zero at the bottom and increases uniformly to 20 m s^{-1} at 10 km. These values are close to the "normal" situation in the troposphere in winter over continents.

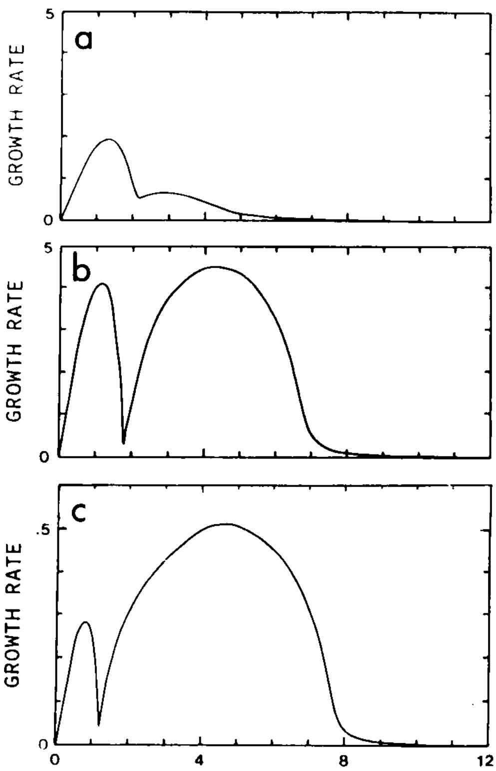

Fig. 6. The growth rate spectrum for (a) an environment without rapidly developing of cyclone where $S_1 = 1.0$, $S_2 = 1.21$, $\lambda_1 = 1.0$, $\lambda_2 = 1.0$, $K = 0.0$, $\delta = 0.1$ and $H = 0.3$, (b) a favorable environment for explosive cyclogenesis where $S_1 = 0.7$, $S_2 = 2.0$, $\lambda_1 = 1.5$, $\lambda_2 = 2.0$, $K = 0.0$, $\delta = 0.01$ and $H = 0.3$, and (c) same as (b) except for $S_2 = 4.0$.

Fig. 6b gives an example of a favorable environment for explosive development of maritime cyclones. The parameter set is: $S_1 = 0.7$, $S_2 = 2.0$, $\lambda_1 = 1.5$, $\lambda_2 = 2.0$, $\delta = 0.01$, and $H = 0.3$. The smallness of δ may be due to both reduced Ekman dissipation and low-level static stability. The growth rate of the most unstable short wave is 0.45 which corresponds to an e-folding time of 1.3 days, which is three times larger than the control case. The wavenumber of the most unstable short wave is about 4.2 which corresponds to a wavelength of 1,500 km. This wavelength has the zonal scale of observed explosive cyclones, i.e., 1,000–2,000 km. The most unstable long wave has the growth rate of 0.41 which corresponds to an e-folding time of 1.4 days. Its wavenumber is 1.1 which corresponds to a wavelength of 5,700 km or about 5 waves around the latitude circle at 45°N. The dimensional height of the interface is 3 km. The low-level static stability, $S_1 = 0.7$, corresponds to a lapse rate of 7.7 K km^{-1}. The upper-level static stability, $S_2 = 2.0$, corresponds to a lapse rate of 3.8 K km^{-1}. The low-level shear, $\lambda_1 = 1.5$, corresponds to a shear of 3 m s^{-1} km^{-1} with the mean zonal speed of 9 m s^{-1} at the height of 3 km. The upper-level shear, $\lambda_2 = 2.0$, corresponds to a shear of 4 m s^{-1} km^{-1} with the mean zonal speed of 37 m s^{-1} at the height of 10 km.

Comparing Figs. 6a and 6b, the above favorable environment for explosive cyclogenesis could be understood as follows. The low-level shear is enhanced by 50% due to the enhanced north-south gradient of sea surface temperature. The low-level static stability is reduced by 30% (due to diabatic heating which alters the environment). The upper-level static stability is increased by 66% due to descending upper-level, cold, dry air, because the adiabatic heating of the descending air reduces the lapse rate in the upper-level. These three factors are favorable for the development of short waves (see Figs. 2a, 3a, b). Although the large upper-level static stability reduces the growth rate of long waves, the large shear in the upper-level may cause the growth rate of the most unstable long wave to be compatible with that of the most unstable short wave (see Fig. 2b).

The effect of upper-level static stability on the development of low-level short wave should not be overlooked. The larger the upper-level static stability, the larger the growth rate of the most unstable short wave (see Fig. 3b). Fig. 6c illustrates such an example (same parameters as those in Fig. 6b except for $S_2 = 4.0$). The growth rate of the most unstable short wave is about 0.51 and corresponds to an e-folding time of 1.14 days, which is larger than that in Fig. 6b. The wavenumber of the most unstable wave is about 4.5 which corresponds to a wavelength of 1,400 km. The upper-level static stability, $S_2 = 4.0$, corresponds to a lapse rate of about zero, implying a deep upper layer with nearly constant temperature in the vertical which results from a substantial descent of upper dry air, or the invasion of stratospheric air. Uccellini et al. (1985) found that stratospheric dry cold air with high static stability could penetrate down to 700 mb during tropopause folding, and that tropopause folding could be a favorable factor for the rapid development of the Presidents' Day cyclone of 18–19 February 1979.

The wave structures of the most unstable short and long waves, $k_{ms} = 4.2$ and $k_{mp} = 1.1$, under the parameters for Fig. 6b are illustrated in Fig. 7. Fig. 7a shows the wave amplitudes as functions of height. The short-wave amplitude has a maximum at the bottom, and decreases dramatically with height, its amplitudes at $z = 0.5$ and $z = 1$ are only about $\frac{1}{6}$ and $\frac{1}{50}$ of that at $z = 0$, respectively. The variation of the long wave amplitude is similar with that in the one-layer Eady model, i.e., it is almost symmetric about $z = 0.5$ where the minimum is observed, and the maximum at the top is slightly larger than that at the bottom. The long wave amplitude at $z = 0.5$ is more than $\frac{1}{2}$ of those at the top and bottom. These results are consistent with those of Staley and Gall (1977) and Blumen (1979), i.e., the short wave is mainly confined to the lower layer while the long wave extends through the depth. Thus, the upper level is controlled by the long wave, while the lower level is affected by both short and long waves. Fig. 7b shows the phase variations with height. Both wave phases tilt westward with height, but the short wave tilt is confined to the lower layer. The phase speeds of the long and short waves are calculated as $c_{rp} = 0.87$ and $c_{rs} = 0.37$, respectively, i.e., the long wave travels eastward faster than the short wave. It is anticipated that when the eastward travelling, developing long wave trough catches up with the developing short wave trough, which could

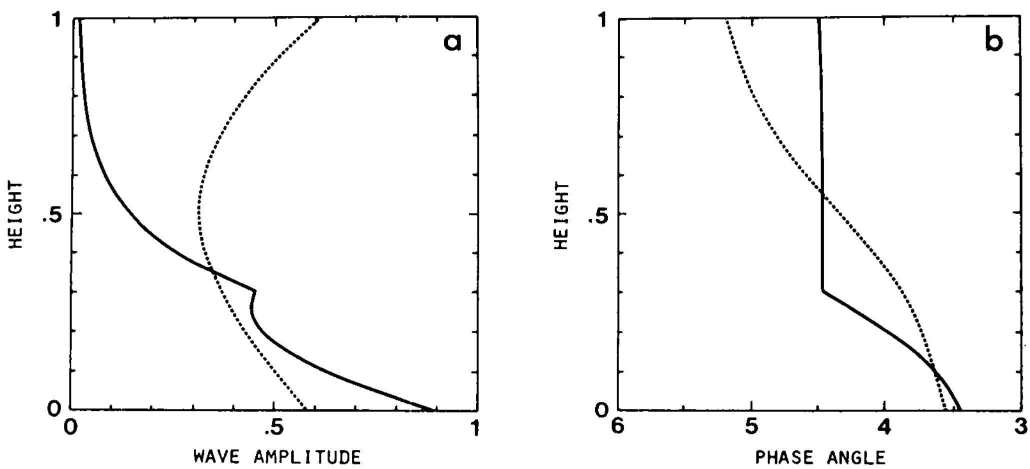

Fig. 7. Vertical wave structures of the most unstable short and long waves: (a) wave amplitude, and (b) phase angle, plotted so that the increase of phase angle with height implies westward tilt with height. Solid and dashed lines denote the short and long waves, respectively.

happen at both the surface and the mid-depth almost simultaneously as shown in Fig. 7b, the system will drastically develop by superposition of the lows of the two waves. The surface low center is about $\frac{1}{4}\pi$ ahead of the upper-level long-wave trough, i.e., about one-quarter of the distance from the trough to the preceding ridge, or about 700 km downstream from the mobile trough at the height of 5 km in the model atmosphere, in which the wavelength of the long wave is about 5,700 km. This favorable situation for explosive cyclogenesis is very close to that found by Sanders and Gyakum (1980) in their synoptic-dynamic climatological analyses.

5. Summary

The occurrence of an explosive cyclone is a combination of baroclinic instability with various favorable conditions. Besides the latent heat release, which is not discussed in this work, many factors are important for the development of explosive cyclones. Table 1 summarizes the effects of changing different parameters on wavenumbers and growth rates of the most unstable short and long waves. An enhanced low-level shear, a reduced low-level static stability, a relatively large upper-level static stability, and an appropriated height of the interface are favorable for the short-wave development. An enhanced upper-level shear and a relatively small upper-level static stability are favorable for the long-wave development; these effects tend to work against the development of the short wave. A small Ekman dissipation which means a relative smoothness of the underlying surface (ocean) is favorable for the development of both short and long waves, compared with a large Ekman dissipation of a rough underlying surface (land). Newtonian form sensible heating does not directly enhance the development of both short and long waves.

The long wave dominates at the upper-level and moves eastward faster than the short wave which is confined to the lower layer. The explosive cyclogenesis may occur when the long wave catches up with the short wave and these fast developing waves are nearly in phase at the surface and the mid-depth. At that time, the surface low is about $\frac{1}{4}\pi$ ahead of the upper-level long wave trough.

Since many explosive cyclogenesis may be involved in the development of both short and long waves, as well as the relative phase of the upper-level trough with respect to the low-level cyclone, the most favorable environment for explosive cyclogenesis may not be expressed by a single parameter, but rather by a combination of several parameters. The effects of some parameters on

Table 1. *Effects of changing of parameters on the growth rates and wavenumbers of the most unstable short and long waves*

Changing of parameters	Short waves		Long waves	
	k_{ms}	$k_{ms}c_i$	k_{mp}	$k_{mp}c_i$
increasing λ_1	slightly increasing	increasing	insensitive	slightly increasing
increasing λ_2	insensitive	decreasing	slightly increasing	increasing
reducing S_1	increasing	increasing	insensitive	insensitive
increasing S_2	increasing	increasing	decreasing	decreasing
decreasing H (for $S_1 < S_2$ or $\lambda_1 > \lambda_2$)	greatly increasing	insensitive	insensitive	insensitive
decreasing δ	increasing	increasing	increasing	increasing
increasing K	increasing	slightly decreasing	insensitive	slightly decreasing

short and long waves are intricate. To find an ideal environment for explosive cyclogenesis, we should pay attention to the parameters favorable for the development of both short wave and long wave, because some of these will tend to enhance one wave at the expense of the other. The nonlinear interaction between the short and long waves, not dealt with here, may also play a rôle. A further nonlinear study of explosive cyclogenesis in the presence of an upper-level planetary trough is under consideration.

6. Acknowledgement

We wish to thank Professor Frederick Sanders for helpful discussions. This work was supported by the Division of Atmospheric Sciences/Experimental Meteorology and Weather Modification of the National Science Foundation under grant ATM-8418624. We gratefully acknowledge this support. This is a contribution no. 240 of the Geophysical Fluid Dynamics Institute, Florida State University, USA.

7. Appendix

The dispersion relation is

$$F(c) = a_{10}(c) - \frac{a_2(c)}{a_1(c)} a_9(c) - \frac{a_5(c)}{a_6(c)}\left[a_8(c) - \frac{a_4(c)}{a_3(c)} a_7(c)\right] = 0,$$

where

$$a_1 = \lambda_1 a_0,$$

$$a_2 = \mu_1(c + c_H) + \frac{c_H}{H}\left[I_s(0)\cosh\left(\frac{\mu_1}{\lambda_1}c\right) + I_c(0)\sinh\left(\frac{\mu_1}{\lambda_1}c\right)\right],$$

$$a_3 = \mu_2 T_2[\lambda_1 H + \lambda_2(1 - H) - c] - \lambda_2,$$

$$a_4 = \mu_2[\lambda_1 H + \lambda_2(1 - H) - c] - \lambda_2 T_2,$$

$$a_5 = -\frac{a_2}{a_1} + T_{1H} + \frac{c_H}{a_0 \lambda_1 H}\left\{I_s(H)\left[\cosh\left(\frac{\mu_1}{\lambda_1}c\right) - T_{1H}\sinh\left(\frac{\mu_1}{\lambda_1}c\right)\right] - I_c(H)\left[T_{1H}\cosh\left(\frac{\mu_1}{\lambda_1}c\right) - \sinh\left(\frac{\mu_1}{\lambda_1}c\right)\right]\right\}$$

$$a_6 = T_{2H} - \frac{a_4}{a_3},$$

$$a_7 = \alpha^{-2}[(\lambda_1 H - c)\mu_2 T_{2H} - \lambda_2],$$

$$a_8 = \alpha^{-2}[(\lambda_1 H - c)\mu_2 - \lambda_2 T_{2H}],$$

$$a_9 = (\lambda_1 H - c)\mu_1 T_{1H} - \lambda_1,$$

$$a_{10} = (\lambda_1 H - c)\mu_1(1 + a_{11}) - \lambda_1(T_{1H} + a_{12}),$$

$$a_{11} = \frac{c_H}{a_0 \lambda_1 H}\left\{I_s(H)\left[T_{1H}\cosh\left(\frac{\mu_1}{\lambda_1}c\right) - \sinh\left(\frac{\mu_1}{\lambda_1}c\right)\right] - I_c(H)\left[\cosh\left(\frac{\mu_1}{\lambda_1}c\right) - T_{1H}\sinh\left(\frac{\mu_1}{\lambda_1}c\right)\right]\right\},$$

$$a_{12} = \frac{c_H}{a_0 \lambda_1 H}\left\{I_s(H)\left[\cosh\left(\frac{\mu_1}{\lambda_1}c\right) - T_{1H}\sinh\left(\frac{\mu_1}{\lambda_1}c\right)\right] - I_c(H)\left[T_{1H}\cosh\left(\frac{\mu_1}{\lambda_1}c\right) - \sinh\left(\frac{\mu_1}{\lambda_1}c\right)\right]\right\},$$

$$T_{1H} = \tanh(\mu_1 H),$$

$$T_{2H} = \tanh(\mu_2 H),$$

$$T_2 = \tanh \mu_2.$$

The relations between A_1, B_1, A_2 and B_2 are as follows:

$$A_1 = -\frac{a_2}{a_1} B_1,$$

$$A_2 = -\frac{a_4}{a_3} B_2,$$

$$B_2 = \frac{a_5 \cosh(\mu_1 H)}{a_6 \cosh(\mu_2 H)} B_1.$$

REFERENCES

Anthes, R. A., Kuo, Y. H. and Gyakum, J. R. 1983. Numerical simulations of a case of explosive marine cyclogenesis. *Mon. Wea. Rev. 111*, 1174–1188.

Blackmon, M. L. 1976. A climatological spectral study of the 500 mb geopotential height of the Northern Hemisphere. *J. Atmos. Sci. 33*, 1607–1623.

Blumen, W. 1979. On short-wave baroclinic instability. *J. Atmos. Sci. 36*, 1925–1933.

Danard, M. B. and Ellenton, G. E. 1980. Physical influences on east coast cyclogenesis. *Atmos.-Ocean. 18*, 65–82.

Fisher, P. W. and Wiin-Nielsen, A. 1971. On baroclinic instability of ultra-long waves. *Tellus 23*, 269–284.

Frederiksen, J. S. 1979. The effects of long planetary waves on the regions of cyclogenesis: linear theory. *J. Atmos. Sci. 26*, 195–204.

Gyakum, J. R. 1983. On the evolution of the *QE II* storm. II: Dynamic and thermodynamic structure. *Mon. Wea. Rev. 111*, 1156–1173.

Haltiner, G. J. 1965. The effects of sensible heat exchange on the dynamics of baroclinic waves. *Tellus 19*, 183–198.

Hanson, H. P. and Long, B. 1984. Climatology of cyclogenesis over the East China Sea. *Mon. Wea. Rev. 113*, 697–707.

Hoskins, B. J. 1971. Atmospheric frontogenesis models: some solutions. *Q. J. R. Meteorol. Soc. 97*, 139–153.

Mansfield, D. A. 1974. Polar lows: the development of baroclinic disturbances in cold air outbreaks. *Q. J. R. Meteorol. Soc. 100*, 541–554.

Min, K. D. and Horn, L. H. 1974. The generation of available potential energy by sensible heating along the east coasts of Asia and North America. *J. Meteorol. Soc. Japan 53*, 204–217.

Mullen, S. L. 1983. Explosive cyclogenesis associated with cyclones in polar air streams. *Mon. Wea. Rev. 111*, 1537–1553.

Murty, T. S., McBean, G. A. and McKee, B. 1983. Explosive cyclogenesis over the northeast Pacific Ocean. *Mon. Wea. Rev. 111*, 1131–1135.

Petterson, A. 1956. *Weather analysis and forecasting, vol. 1, Motion and motion systems*. McGraw-Hill, 428 pp.

Rasmussen, E. 1979. The polar low as an extratropical CISK disturbance. *Q. J. R. Meteorol. Soc. 105*, 531–549.

Roebber, P. J. 1984. Statistical analysis and updated climatology of explosive cyclones. *Mon. Wea. Rev. 112*, 1577–1589.

Rogers, E. and Bosart, L. F. 1986. An investigation of explosively deepening oceanic cyclones. *Mon. Wea. Rev. 114*, 702–718.

Saito, N. 1977. On the structure of medium-scale depressions over the East China Sea during AMTEX75. *J. Meteorol. Soc. Japan 55*, 286–300.

Sanders, F. and Gyakum, J. R. 1980. Synoptic-dynamic climatology of the "bomb". *Mon. Wea. Rev. 108*, 1589–1606.

Staley, D. O. and Gall, R. L. 1977. On the wavelength of maximum baroclinic instability. *J. Atmos. Sci. 34*, 1679–1688.

Uccellini, L. W., Keyser, D., Brill, K. F. and Wash, C. H. 1985. The Presidents' Day cyclone of 18–19 February 1979: influence of upstream trough amplification and associated tropopause folding on rapid cyclogenesis. *Mon. Wea. Rev. 113*, 962–988.

Winston, J. S. 1965. Physical aspects of rapid cyclogenesis in the Gulf of Alaska. *Tellus 7*, 481–500.

Wang, B. and Barcilon, A. 1986. Moist stability of a baroclinic zonal flow with conditionally unstable stratifications. *J. Atmos. Sci. 43*, 705–719.